

Supporting Information for

Controllable Synthesis of MnO₂ Nanostructure Anchored on Graphite Foam with Different Morphology for High-Performance Asymmetric Supercapacitor

Xingbin Lv^a, Hualian Zhang^a, Feifei Wang^a, Zhufeng Hu^a, Yuxin Zhang^c, Lili Zhang^{b,}, Rui Xie^a, Junyi Ji^{a,d,*}*

^aSchool of Chemical Engineering, Sichuan University, Chengdu, Sichuan 610065, China. E-mail: junyiji@scu.edu.cn

^bInstitute of Chemical and Engineering Sciences, A*STAR, 1 Pesek Road, Jurong Island, 627833 Singapore. E-mail: zhang_lili@ices.a-star.edu.sg

^c College of Material Science and Engineering, Chongqing University, Chongqing, 400044, P. R. China

^dState Key Laboratory of Polymer Materials Engineering, Sichuan University, Chengdu, Sichuan, 610065, P. R. China

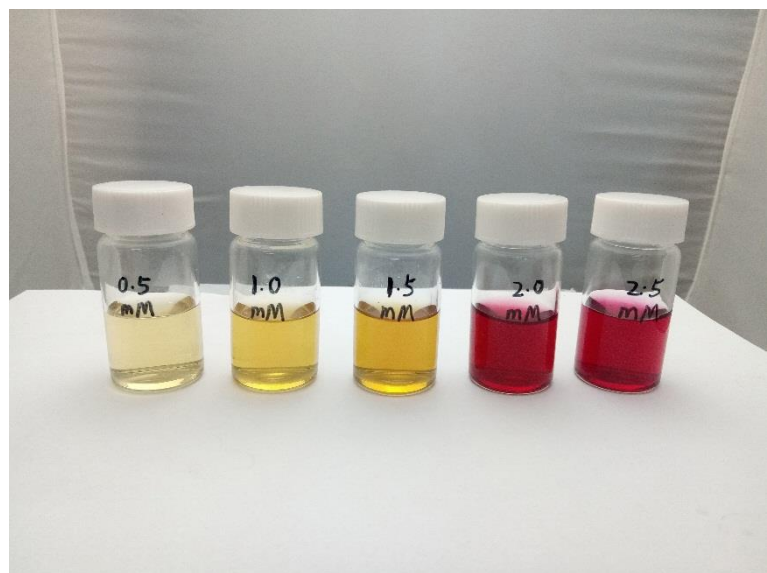


Figure S1. The digital photograph of the solution collected after hydrothermal reaction.

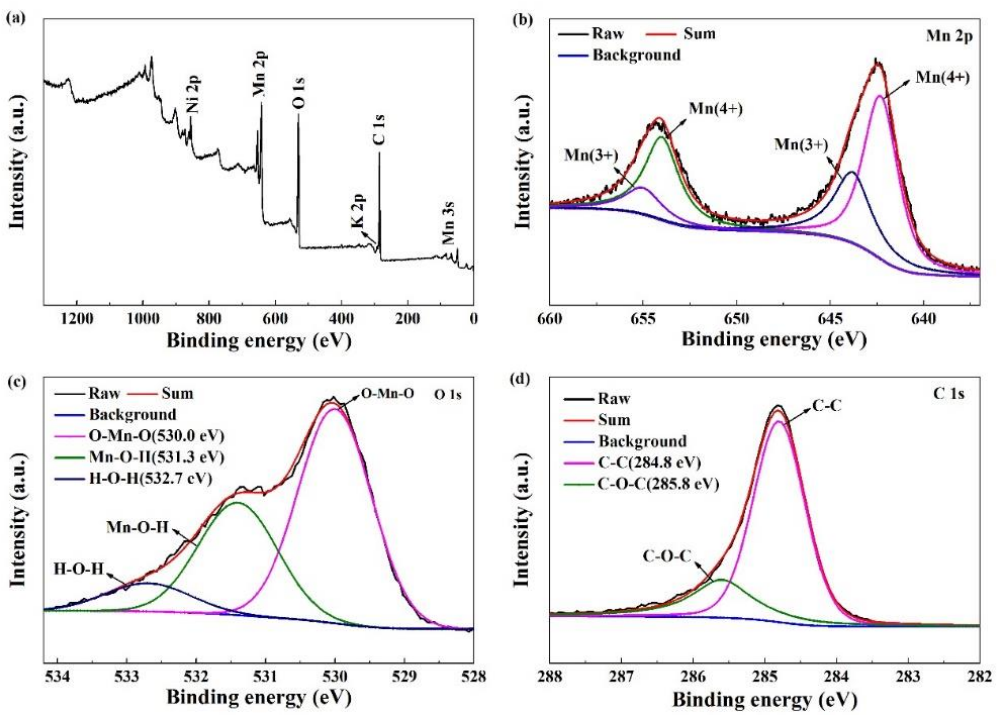


Figure S2. XPS spectrum of the $\text{MnO}_2/\text{GNF-0.5}$ composite, (a) full survey spectrum, (b) Mn 2p spectrum, (c) O 1s spectrum, (d) C 1s spectrum.

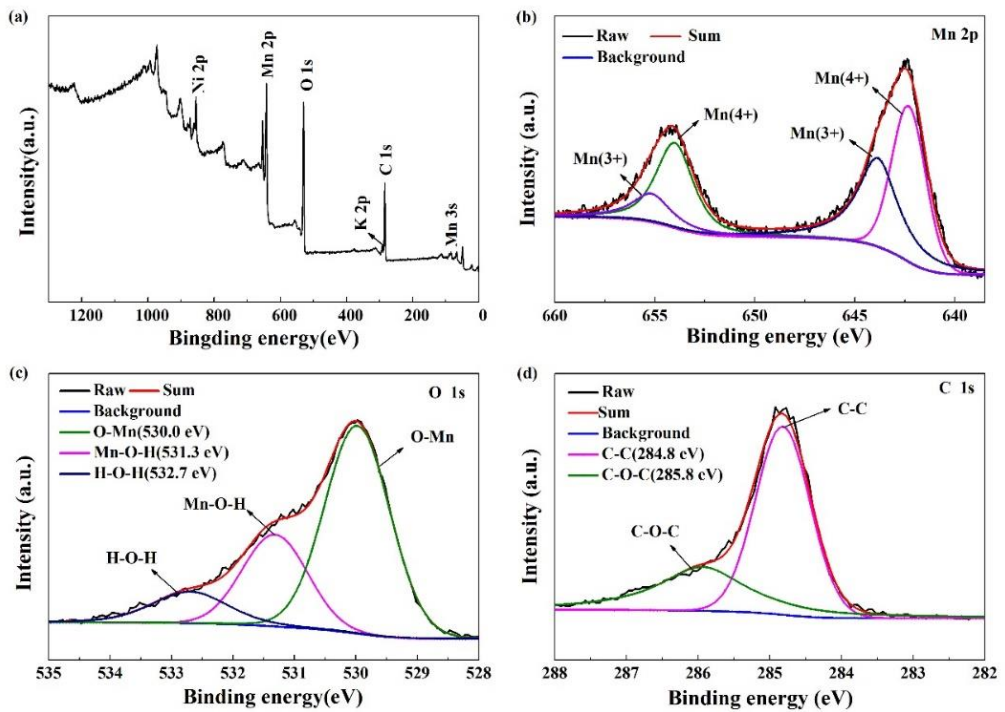


Figure S3. XPS spectrum of the $\text{MnO}_2/\text{GNF-1.0}$ composite, (a) full survey spectrum, (b) Mn 2p spectrum, (c) O 1s spectrum, (d) C 1s spectrum.

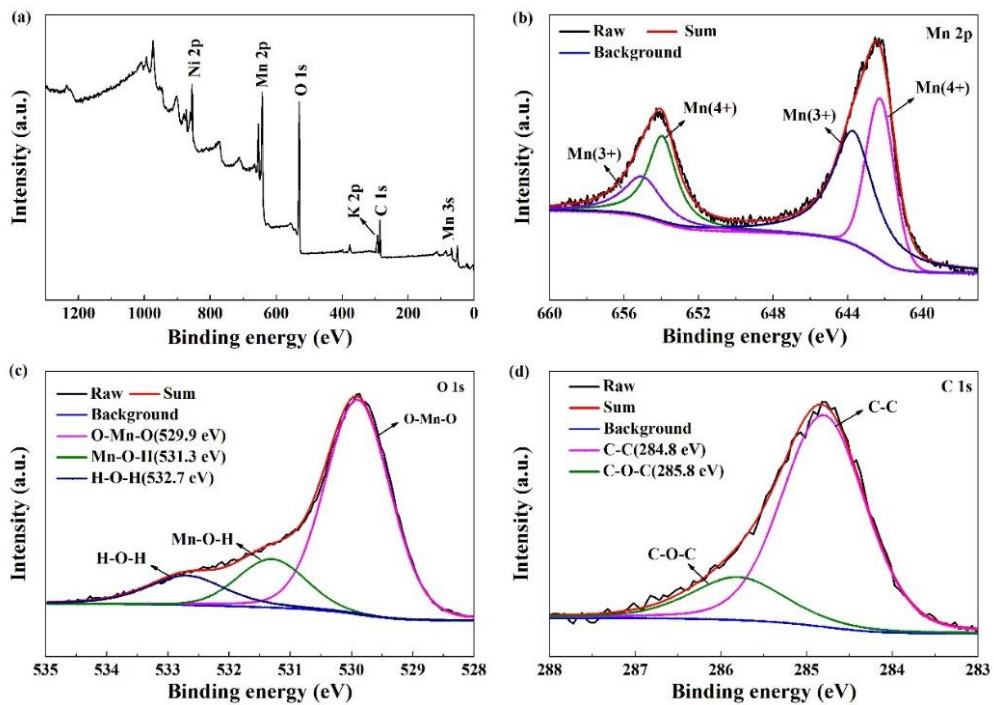


Figure S4. XPS spectrum of the $\text{MnO}_2/\text{GNF-2.0}$ composite, (a) full survey spectrum, (b) Mn 2p spectrum, (c) O 1s spectrum, (d) C 1s spectrum.

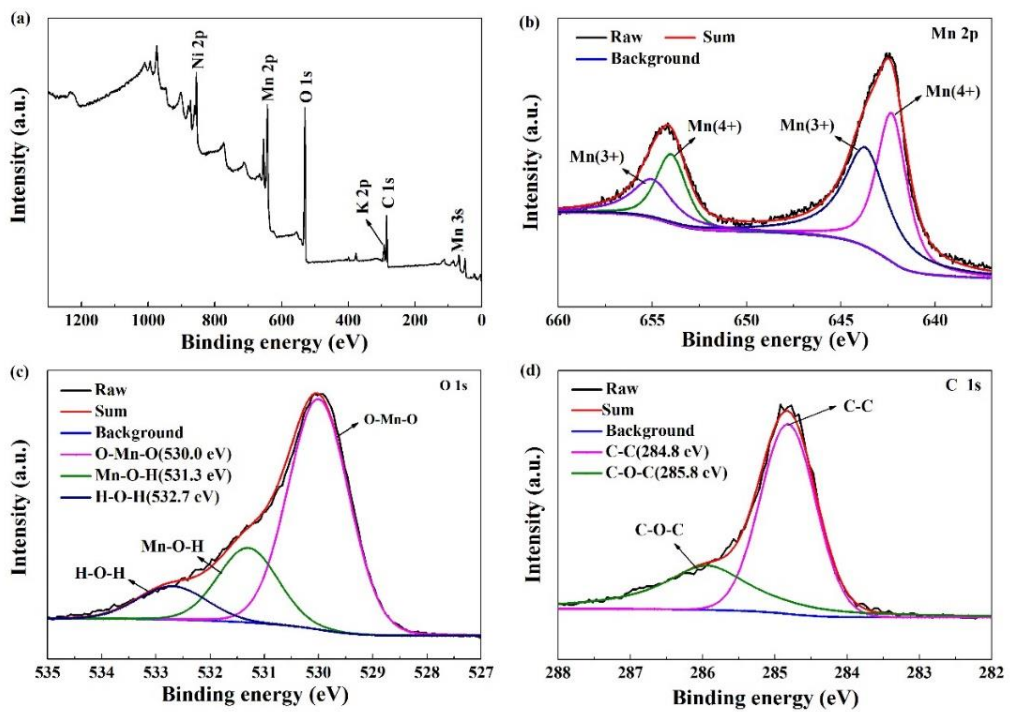


Figure S5. XPS spectrum of the $\text{MnO}_2/\text{GNF-2.5}$ composite, (a) full survey spectrum, (b) Mn 2p spectrum, (c) O 1s spectrum, (d) C 1s spectrum.

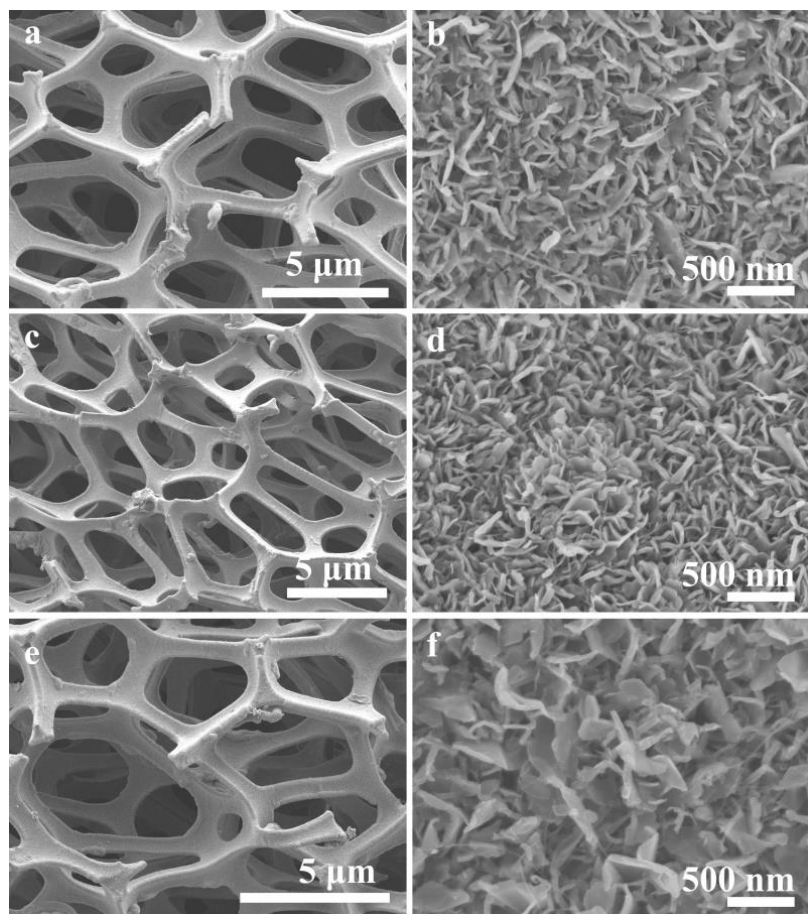


Figure S6. SEM images of MnO₂ anchored on the nickel foam (NF) substrate, the growth parameter is the same as that of the MnO₂/GNF composites. (a, b) MnO₂/NF-0.5, (c, d) MnO₂/NF-1.5 and (e, f) MnO₂/NF-2.5.

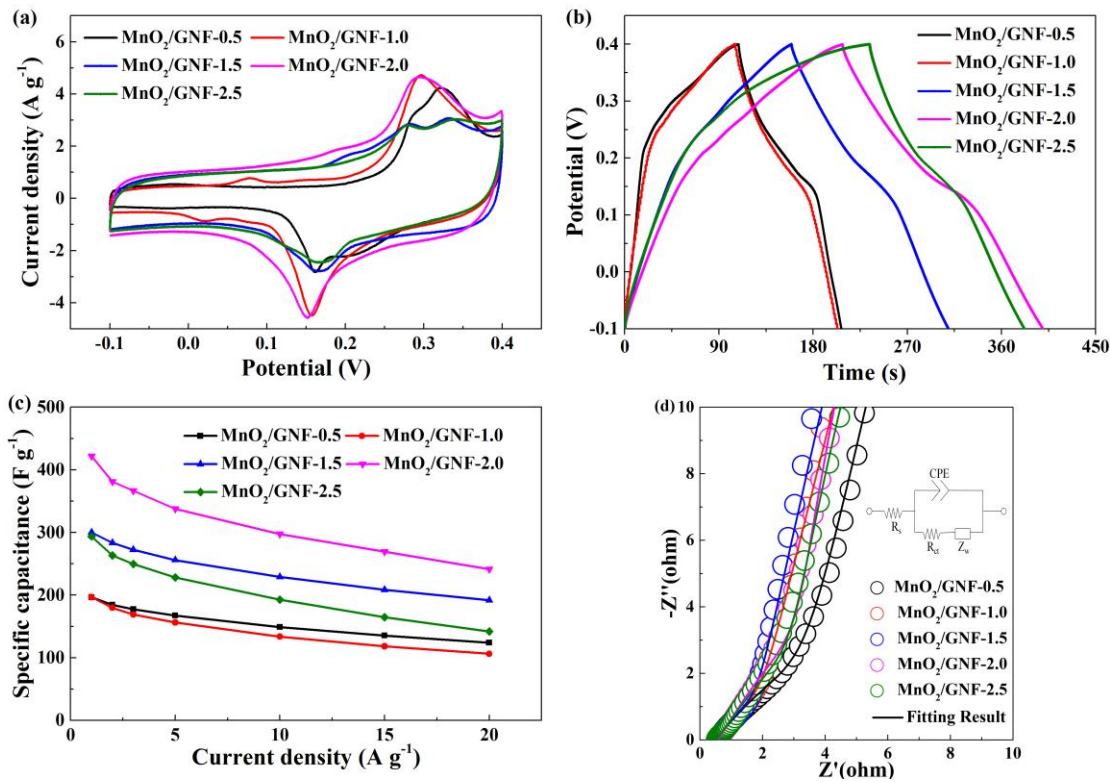


Figure S7. The electrochemical performance of MnO₂/GNF samples measured in 6 M KOH solution. (a) CV curves of MnO₂/GNF samples at a scan rate of 5 mV s^{-1} , (b) galvanostatic charge/discharge profiles of MnO₂/GNF samples at a current density of 1 A g^{-1} , (c) rate performance of MnO₂/GNF samples at various current densities and (d) Nyquist plots and corresponding fitting results of MnO₂/GNF samples, the inset shows the equivalent circuit.

6 M KOH was also used as the electrolyte to study the electrochemical properties of MnO₂/GNF electrodes in a three-electrode system. CV curves in **figure S7a** indicates a pair of redox peaks located at 0.15 and 0.3 V, respectively, which can be attributed to the redox transition between Mn(III) and Mn(IV).¹ The GCD curves of MnO₂/GNF electrodes at a current density of 1 A g^{-1} in the potential range of -0.1 to 0.4 V are shown in figure S7b. The redox reaction is also reflected by a non-triangular shape of GCD curve. The MnO₂/GNF-2.0 electrode shows the highest specific capacitance of 422 F g^{-1} , and a 71% capacitance retention can be achieved when the current density

increase from 1 to 10 A g⁻¹ (Figure S7c). This value is much better than previous reported works, such as the hierarchical birnessite-type MnO₂ nanoflowers (138 F g⁻¹ at 10 A g⁻¹),² the honeycomb MnO₂ nanospheres/carbon nanoparticles/graphene composites (170 F g⁻¹ at 10 A g⁻¹) and the well-defined MnO₂ nanorod (201 F g⁻¹ at 5 A g⁻¹).^{3,4} Moreover, a capacitance retention of 90% was obtained for MnO₂/GNF-2.0 electrode after 1000 cycles (**Figure S8**), which is slightly lower than in neutral electrolyte. Moreover, the structure of MnO₂/GNF-2.0 sample was maintained well during the charge/discharge cycling process (inset in figure S8). Additionally, the MnO₂/GNF -2.0 electrode presents a small charge transfer resistance (R_{ct}) and Warburg resistance(R_w), indicating good electrochemical performance of MnO₂/GNF-2.0 sample as a supercapacitor electrode material (Figure S7d and Table S3).

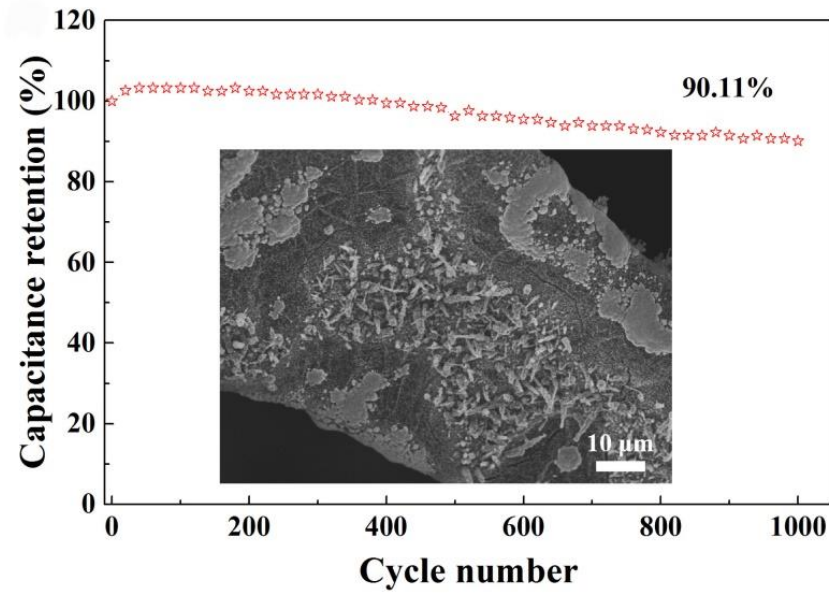


Figure S8. Cycling performance of the MnO₂/GNF-2.0 electrode measured at a current density of 10 A g⁻¹ in 6 M KOH electrolyte, the inset is the SEM image of the electrode after 1000 cycling.

Table S1 The detailed elemental compositions of the different composites.

Samples	C (at.%)	O (at.%)	Mn (at.%)	K (at.%)	K/Mn (%)
MnO ₂ /GNF-0.5	51.961	33.654	13.598	0.787	5.788
MnO ₂ /GNF-1.0	40.986	41.600	15.948	1.465	9.185
MnO ₂ /GNF-1.5	33.238	45.831	18.369	2.561	13.942
MnO ₂ /GNF-2.0	26.688	48.28	20.516	4.517	22.017
MnO ₂ /GNF-2.5	32.689	45.784	17.899	3.628	20.270

Table S2 Average diameter/thickness of the nanowires/nanosheets collected from the SEM images of the different samples.

Samples	Loading mass(mg/cm ⁻²)	Nanowires (nm)	Nanosheets (nm)
MnO ₂ /GNF-0.5	0.5	12	--
MnO ₂ /GNF-1.0	0.6	22	--
MnO ₂ /GNF-1.5	0.9	17	17
MnO ₂ /GNF-2.0	1.5	--	17
MnO ₂ /GNF-2.5	2.0	--	26

Table S3. Fitting results for electrochemical impedance spectroscopy.

Electrolyte	Samples	R _s (Ω)	R _{ct} (Ω)	CPE
1 M Na₂SO₄	MnO ₂ /GNF-0.5	1.75	0.35	0.709
	MnO ₂ /GNF-1.0	2.092	0.25	0.733
	MnO ₂ /GNF-1.5	2.398	0.28	0.709
	MnO ₂ /GNF-2.0	2.046	0.342	0.686
	MnO ₂ /GNF-2.5	2.582	0.31	0.69
6 M KOH	MnO ₂ /GNF-0.5	0.57	0.329	0.797
	MnO ₂ /GNF-1.0	0.546	0.38	0.747
	MnO ₂ /GNF-1.5	0.553	0.42	0.758
	MnO ₂ /GNF-2.0	0.577	0.444	0.709
	MnO ₂ /GNF-2.5	0.529	0.455	0.681

REFERENCES:

- 1 M. Huang, X. Zhao, F. Li, L. Zhang and Y. Zhang, *J. Power Sources*, **2015**, 277, 36-43.
- 2 S. Zhao, T. Liu, D. Hou, W. Zeng, B. Miao, S. Hussain, X. Peng and M. S. Javed, *Appli. Surf. Sci.*, **2015**, 356, 259-265.
- 3 Y. Xiong, M. Zhou, H. Chen, L. Feng, Z. Wang, X. Yan and S. Guan, *Appli. Surf. Sci.*, **2015**, 357, 1024-1030.
- 4 N. Li, X. Zhu, C. Zhang, L. Lai, R. Jiang and J. Zhu, *J. Alloys Compd.*, **2017**, 692, 26-33.